BIOSCIENCES BIOTECHNOLOGY RESEARCH ASIA, June 2024. Vol. **21**(2), p. 555-567

Control of Small GTPase Ras Using a Calmodulin-based Ionochromic Nanodevice

Ziyun Zhang, Yassine Sabek and Shinsaku Maruta*

Division of Bioinformatics, Graduate School of Engineering,
Soka University, Hachioji, Tokyo, Japan.

http://dx.doi.org/10.13005/bbra/3247

(Received: 12 December 2023; accepted: 12 March 2024)

The small GTP-binding protein, HRas, is a switch-like molecule that plays an important role in the regulation of many cell processes. It is activated by binding to GTP and is inactivated when GTP is hydrolyzed to GDP. Ras has two accessory factors, guanine accelerate protein (GAP) and guanine nucleotide exchange factor (GEF), which facilitate its switching function by accelerating GTP hydrolysis and GDP/GTP exchange. Calmodulin (CaM) is a crucial signaling and regulatory molecule involved in many calcium-dependent processes. In the calcium-bound state, CaM binds tightly to the M13 peptide and IQ motif. Because there are no reports using CaM as an ionochromic switch system, CaM was used here to artificially control Ras. An HRas fusion protein with M13 (M13-HRas) was expressed using an established Escherichia coli expression system. M13-HRas showed 73% ion-regulation when the regulatory factors GAP and GEF were present. The CaM-bound state inhibited the interaction between M13-HRas and GST-Raf while maintaining a similar GTPase activity regulation ratio. Finally, the inhibition of CaM binding between M13-HRas and two accessory factors was confirmed. Thus, modifying the G protein functional site with M13 enabled ionochromic control of G protein function with CaM, which has implications for cancer therapy.

Keywords: Calmodulin; Ionochromic; Ras; Small Gtpase.

Biological molecular machines are complex and play a crucial role in regulating cellular processes. These machines are categorized into ATPases and GTPases based on their primary energy sources. Kinesin, myosin, dynein, and chromatin remodeling proteins are well-known ATPases. In previous studies, the photo-reversible control of kinesin Eg5 has been achieved using an azobenzene derivative [1,2]. There are more than 100 GTP-binding proteins in mammalian cells that act as biological timers and regulate various biological processes.

Ras proteins belong to a superfamily of small monomeric GTPases that function as a molecular binary switch [3]. The binary switch behavior of Ras has been shown to be active upon binding to GTP and inactive upon binding to GDP. As the release of GDP and hydrolysis of GTP by Ras are slow (GTP hydrolysis rate constant: 0.028 min^{-1}, GDP dissociation rate constant: 0.079 min^{-1}) [4], the switch-like function is accelerated by interactions with specific protein-binding partners, guanine nucleotide exchange factor (GEF) and

*Corresponding author E-mail: maruta@soka.ac.jp

guanine accelerate protein (GAP). In the Ras–GTP cycle, GEFs promote the release of GDP from Ras, whereas GAPs promote the hydrolysis of GTP inside Ras (Figure 1). Collectively, GEFs and GAPs accelerate the GTP hydrolysis rate by approximately 100,000 times [5].

Ras, via various downstream effector enzymes, regulates cellular signal transduction pathways implicated in cell growth, apoptosis, migration, and differentiation [3,6]. Activated Ras has a high affinity for downstream proteins, such as the serine/threonine kinase Raf. After binding to Ras, Raf activates the mitogen-activated protein kinase (MAPK) extracellular signal-regulated kinase pathway to control cell cycle progression and differentiation [7]. Therefore, the regulation of Ras activity is crucial for controlling cell cycle progression.

Ras expressed in diverse mammalian tissues, which are encoded by three analogous genes: Harvey Ras (HRas), Kirsten Ras (KRas), and neural Ras (NRas)[8]. Ras consists of a G-domain at the N-terminus and a hypervariable region (HVR) at the C-terminus. The G domain contains two switch regions, region '! (30-37 aa) and region a! (60-76 aa), which have GTP and GDP binding ability, enabling Ras to function as a molecular switch. The HVR (167–187 aa) is unstructured and may change Ras from a monomer to a multimer when 2-nitrobenzyl bromide is incorporated into cysteine residues [9]. Hence, in this study, only Ras residues 1–166 were used to reduce unnecessary multiplication.

Chromic compounds possess the unique ability to alter their properties or color response when exposed to various external factors, such as light, temperature, pH changes, ion concentration changes, and other environmental stimuli [10,11]. These changes are classified as photochromic, thermochromic, and ion-responsive and are dependent on the type of environmental alteration. In this study, we specifically focused on ion-responsive compounds that have been utilized in clinical diagnostics and environmental analysis for several years [12]. However, employing ion sensors within cells can be challenging owing to concerns related to solubility, membrane transposability, and cellular toxicity. To address these concerns, we choose to use ion-responsible protein Calmodulin (CaM), the potential use of this molecular device protein was investigated, which has similar ion-responsive properties. It can be expressed from cells and shows no cellular toxicity.

As a crucial protein, CaM plays a pivotal role in numerous biological processes as a calcium sensor. It is relatively small and comprises four EF-hand motifs, with two forming a globular N-terminal domain and the remaining two forming a globular C-terminal domain; these domains are connected by a short, flexible hydrophobic linker[13]. When Ca^{2+} binds to CaM, the hydrophobic linker is exposed, causing a structural shift from a sheet to a helix form[13,14]. CaM is a ubiquitous component of eukaryotic cells that functions in signal transduction pathways. Over 300 known CaM target peptides interact with Ca^{2+} in an intercellular manner, with the majority relying on hydrophobic residues for their binding affinity [15,16]. Among these, the M13 peptide and the IQ motif stand out as prototypical CaM-binding sequences. The IQ motif is notable for its ability to bind with the apo form of calmodulin (CaM) with high affinity, whereas the M13 peptide is distinguished by its high-affinity binding to CaM in a Ca^{2+}-dependent manner [13,17,18]. Intrinsic fluorescence analysis reveals that the binding between CaM and the M13 peptide reaches saturation at a 1:1 molecular ratio [19,20]. Furthermore, the strength of the interaction between CaM and the M13 peptide is comparable to that of the intact enzyme, highlighting the functional significance of this binding in cellular processes [17].

In a noteworthy development, a recent study by Hideki et al. has demonstrated the reversible control of cargo attachment to a molecular shuttle, achieved by fusing the K560 peptide with CaM. This innovative approach utilized changes in Ca^{2+} concentration to modulate the binding and release of cargo molecules, showcasing the potential for CaM and its interacting peptides in the development of dynamic, responsive biological systems [20].

In this study, we aimed to develop an ionochromic nanodevice capable of serving as a molecular switch for applications in factory processing. To achieve this, we engineered a Ras-based molecular machine designed to toggle between active ("ON") and inactive ("OFF") states in response to calcium ion levels. Specifically, the

device maintains the Ras protein in an "ON" state in the absence of Ca^{2+} and switches it to an "OFF" state upon Ca^{2+} presence.

To construct this molecular switch, we incorporated the M13 peptide into the N-terminus of the Ras protein by designing a fusion Ras protein. This strategic modification allowed us to harness the ion sensitivity of the M13 peptide, thereby enabling the artificial control of the Ras protein's activity state. Through the application of this fusion protein, we demonstrated the feasibility of ion regulation control over the Ras fusion proteins' activity. Furthermore, we successfully extended this ion control mechanism to modulate the interaction between Ras and its downstream effector protein, Raf, showcasing the potential of our ionochromic nanodevice in controlling molecular-level switches in a factory setting.

MATERIALS AND METHODS

Construction of expression vectors

Fusion HRas protein (M13-HRas (N)) was created for this study. To create M13-HRas, the HRas catalytic domain was positioned on the C-terminal side, and the M13 peptide was placed on the N-terminal side. To avoid steric hindrance, a GS linker (LESGGSGGGS) was incorporated into each interval of HRas and M13 peptides.

Dr. Sako (RIKEN) kindly provided the cDNA of human H-Ras WT (1–189) and GST-cRaf (RBD)-His, which were amplified using polymerase chain reaction (PCR) and ligated into the pET42c vector. Plasmids for the HRas catalytic domain (residues 1–166) were also constructed, where 23 amino acids from the C-terminus were eliminated and then amplified using PCR. To create M13-HRas, the M13-GS linker was inserted into HRas (1–166) using a Q5 Site-Directed Mutagenesis Kit (BioLabs Japan, Inc.). Previously described protocols were used to prepare cDNA for GEF (Son of sevenless homologue 1 (Sos1) cat 564–1049 aa) and GAP (type I neurofibromatosis (NF1) GTPase-activating protein-related domain 1195–1528 aa) [9].

Expression and purification of recombinant proteins

The recombinant protein M13-HRas was incorporated into the pET21a plasmid (Novagen, Madison, WI, USA). Subsequently, these plasmids transformed *Escherichia coli (E. coli)* Rosetta2(DE3) pLysS cells for expression. The expressed proteins, featuring a 6x His tag (as illustrated in Fig. 2A), underwent purification through metal chelation column chromatography, employing a Co^{2+}-NTA column, following the manufacturer's instructions.

To ascertain the purity of the proteins, the resulting fractions were scrutinized using sodium dodecyl sulfate-polyacrylamide gel electrophoresis (SDS-PAGE). Post-purification, the proteins were dialyzed into a buffer solution (30 mM Tris–HCl, pH 7.5, 150 mM NaCl, 1 mM $MgCl_2$, and 0.5 mM dithiothreitol) and subsequently stored at -80 ! for future use. These procedural steps were meticulously executed with scientific rigor, ensuring the meticulous preservation of the quality and integrity of the recombinant proteins.

GTPase activity assay

A previously established method was used to evaluate GTPase activity [21,22]. A mixture containing M13-HRas (2.5 ìM), CaM (0 or 2.5 µM), and $CaCl^{2+}$/EGTA (0.5 mM) in GTPase activity assay buffer (30 mM Tris-HCl pH 7.5, 120 mM NaCl, and 2 mM $MgCl_2$) was prepared. The mixture was pre-incubated for 5 min in the presence of 2.5 ìM Sos and NF1. Next, 1 mM GTP was added to initiate the GTPase assay at 25 ÚC for 30 min. The reaction was stopped by adding 10% trichloroacetic acid. The supernatant was separated using centrifugation for 5 min at 17360 × *g* at 4 ÚC. The BioMol Green Reagent was then mixed with the supernatant and incubated at 25 ÚC for 30 min to determine the amount of inorganic phosphate (Pi) generated by GTP hydrolysis. The Pi concentration was measured at 630 nM using iMark microplate reader (BIO-RAD). The GTPase assay was performed in triplicate, and the results were expressed as the mean ± standard deviation.

GEF/GAP dose dependence assay

The determination of GEF/GAP dose dependence aimed to ascertain the apparent Kd of GEF or GAP in the Ras GTPase assay of M13-HRas (2.5 ìM), CaM (0 or 2.5 µM), and $CaCl^{2+}$/EGTA (0.5 mM). The dose dependence involved GAP doses of 0, 0.3125, 0.625, 1.25, 2.5, and 5 µM, along with GEF doses of 0, 0.625, 1.25, 2.5, 5, 10, 20, and 40 µM. These experiments were conducted following the procedures outlined in the *GTPase activity assay*. Each GTPase assay was

executed in triplicate, and the results were reported as the mean ± standard deviation. The data points were fitted using the saturation curve equation, and the apparent Kd values were estimated from the concentrations of regulators, representing the points where GTPase activity reached half-maximal levels on the saturation curve.

Pulldown assay with effector c-Raf

To investigate the interaction between the Ras fusion protein and its downstream target, cRaf, a pulldown assay was conducted under the manufacturer's instructions. A reaction mixture containing 10 ìM M13-HRas and 1.4 ìM Glutathione-S-Transferase (GST)-tagged c-Raf (RBD) was prepared and added to 30 ìL of glutathione-Sepharose 4B beads within 100 ìL of assay buffer. This buffer was composed of 25 mM HEPES-NaOH (pH 7.5), 150 mM NaCl, 5 mM ethylenediaminetetraacetic acid (EDTA), 0.05% Triton X-100, and 1 mg/mL bovine serum albumin (BSA). The mixture was then incubated at 30 °C for 5 minutes with either 100 ìM GppNHp or GDP to facilitate the nucleotide exchange reaction, which was subsequently terminated by the addition of 10 mM $MgCl_2$. Following the introduction of additional Ca^{2+}/EGTA, the mixture was further incubated at 4 °C for 90 minutes under continuous stirring. Subsequent to this incubation, the resin was washed three times with 400 ìL of wash buffer, which consisted of 25 mM HEPES-NaOH (pH 7.5), 150 mM NaCl, 2 mM $MgCl_2$, 0.05% Triton X-100, and 1 mg/mL BSA. The proteins adhered to the resin were eluted by boiling in SDS sample buffer, which comprised 6.3 mM Tris-HCl, 10% glycerol, 5% â-mercaptoethanol, and 0.25 mg/mL bromophenol blue. The eluted proteins were then subjected to analysis via 10% SDS-PAGE.

Table 1. The affinity of M13-HRas with guanine accelerates protein (GAP) and guanine nucleotide exchange factor (GEF) in the presence of Ca^{2+} and the absence of Ca^{2+} conditions

		$+Ca^{2+}$	$-Ca^{2+}$
GAP-GTPase	Kd (µM)	0.21	0.80
	Vmax (sec^{-1})	0.002	0.006
GEF-GTPase	Kd (µM)	31.80	7.52
	000Vmax (sec^{-1})	0.022	0.022

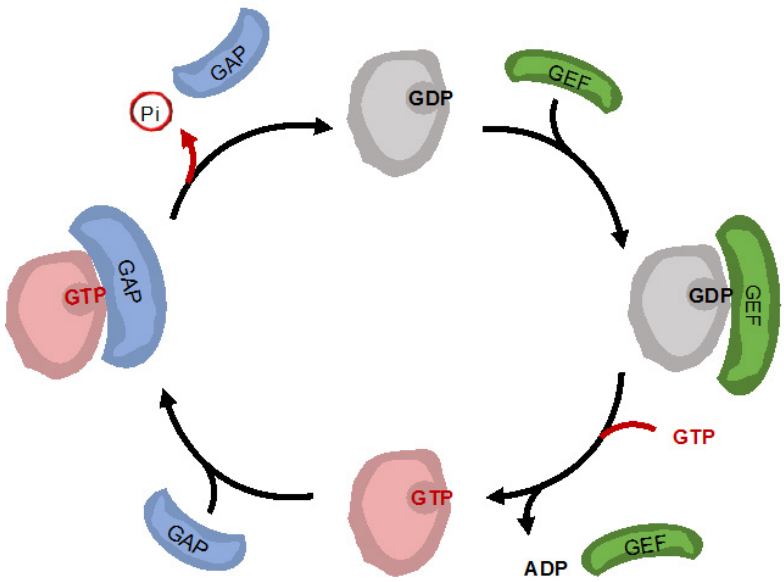

Fig. 1. Small GTPase Ras switching mechanism: Ras behaves as a switch-like biomolecular in intracellular signal transduction. This switch is regulated and accelerated by guanine nucleotide exchange factor: GEFs and GTPase activation proteins: GAPs. GEFs accelerate the exchange of GDP (inactive) to GTP (active), and GAPs accelerate the GTP hydrolysis to become inactive. GEFs expedite the conversion of the inactive GDP to its active GTP counterpart, while GAPs hasten the hydrolysis of GTP, causing it to revert to its inactive state

RESULTS AND DISCUSSION

Design and preparation of M13-HRas

The M13 peptide and the IQ motif are well-known CaM-binding peptides that have been studied for many decades. Although the incorporation of M13 and CaM into kinesin Eg5 to build an ion control drug translator system has been successfully created [20], there are no reports on the use of M13 and CaM to create an ionochromic switch system. To develop a nanodevice that employs the ionochromic protein CaM to regulate Ras function, the fusion proteins M13-HRas were constructed, as depicted in Figures 2A and 2B. M13 was integrated into the N-terminus of HRas. To avoid the influence of the spatial structure of the M13 peptide, an additional GS linker was used. The fusion proteins were produced using an *E. coli* expression system and purified using a cobalt chelate affinity column following the protocols detailed in the Materials and Methods section. The purification results are shown in Figure 3; the molecular weight of HRas (1–166) is 20.8 kDa and the molecular weight of M13-HRas is 25.08 kDa. The purified proteins were then confirmed to have the correct molecular weight using 15% SDS-PAGE, as demonstrated in Figure 3. M13-HRas was compared with the Ras (1–166), and the expected results were observed.

Ionocontrol of the GTPase activity of fusion Ras

As a switch-like GTPase protein, Ras has "on-state" GTP binding and "off-state" GDP binding; both have a group of accelerate cofactors, GAPs, and GEFs, which accelerate the GTPase cycle by approximately 10^5 fold [5,23]. In this study, the GTPase activity of Ras was measured in the presence of NF1 and SOS1. Figure 1 illustrates the Ras GTPase cycle. In this experiment, GTPase activity was measured in the presence of excess GTP and compared to that of the wild-type HRas, which served as a control. As shown in Figure 4, the incorporation of M13 decreases the GTPase activity of M13-HRas by approximately 40% compared to that of the WT HRas. Upon the addition of Ca^{2+}, CaM binds to wild-type M13 with a binding affinity Kd of 0.19

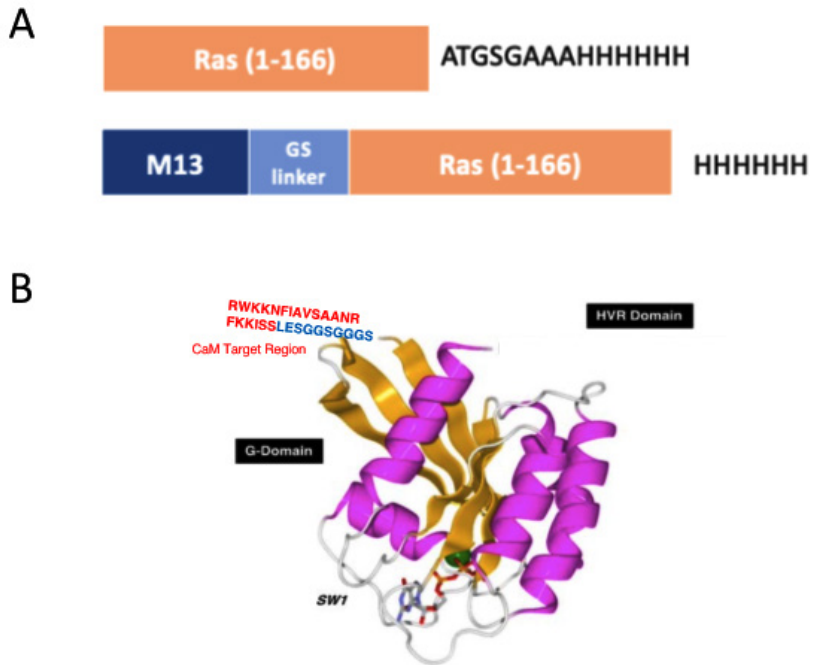

Fig. 2. Design of recombinant proteins: (A) HRas (1-166) and HRas fused with M13 (M13-HRas). The orange part is Ras DNA, light blue is 10aa GS-linker and dark blue is the M13 peptide (20aa). (B) Schematic model of M13-HRas. GS-linker is shown in blue sequence and the M13 peptide is shown in rad sequence connect in the N-terminus of HRas (1-166)

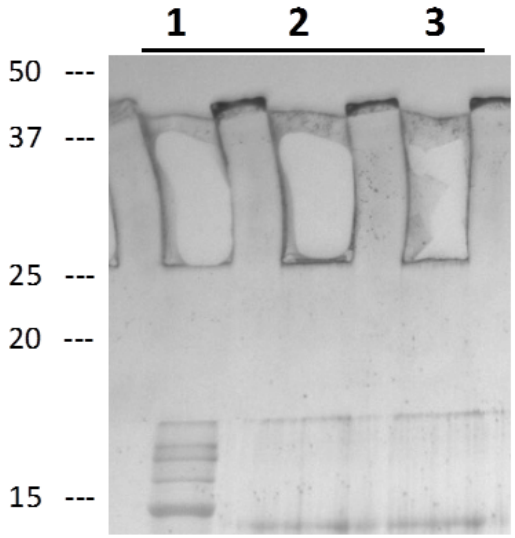

Fig. 3. SDS-PAGE of the fusion Hrass: Purificated HRas (1-166) and M13-HRas was resolved by 15% SDS-polyacrylamide gel stained by Coomassie Brilliant Blue (CBB) -stained containing Standard (lane 1),HRas (1-166) (lane 2) and M13-HRas (lane 3)

nM [24]. In the GTPase activity experiment, CaM and M13-HRas were used at a molecular ratio of 1:1, as described by Hideki [20]. To analyze the ion control of Ras function, the specific GTPase activity of M13-HRas was measured in four states: in the presence of CaM and Ca^{2+}, in the presence of only CaM, in the presence of only Ca^{2+}, and in the absence of CaM and Ca^{2+}, as shown in Figure 5. In the presence of CaM, M13-HRas exhibited a significant difference in GTPase activity in the presence and absence of Ca^{2+}. Specifically, in the presence of Ca^{2+}, the GTPase activity of M13-HRas decreased by 73%. However, comparing the results in the four tested states, even just in the presence of Ca^{2+}, HRas GTPase activity showed an average 25% decrease. According to Buhrman et al. (2010), Ras has a second ion-binding site on the opposite face of the G-domain, specifically binding divalent cations. Additionally, Ca^{2+} is known to allosterically bind to the classical nucleotide-binding site [25,26]. Upon reducing the concentration of Ca^{2+}, our observations indicated a corresponding increase in the GTPase activity of Ras (data not

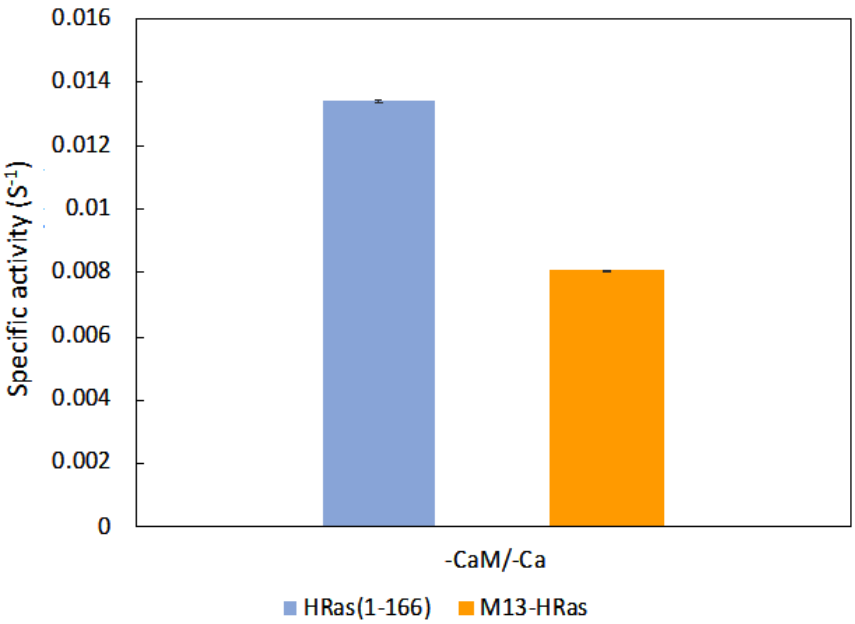

Fig. 4. Specific GTPase activity of M13-HRas and HRas (1-166) at 630 nm within GAP and GEF: GTPase activity of HRas (1-166), M13-HRas was measured at 25 ÚC in a reaction mixture containing 2.5µM HRas, 2.5 µM GAP, 2.5 µM GEF, 30 mM Tris-HCl (pH7.5), 120 mM NaCl, 2mM $MgCl_2$, 1 mM GTP as described previously [10]. The data and standard deviation were derived from three independent experiments.

shown). Therefore, it becomes evident that in the presence of Ca^{2+}, HRas binds with Ca^{2+}, influencing its GTPase activity.

Interestingly, a distinct scenario emerged when CaM was introduced, resulting in a specific 15% increase in GTPase activity. Examining the amino acid sequence of HRas, we identified two isoleucine residues (I21, 24) and two glutamine residues (Q22, 25) close to the HRas switch I region. It is widely acknowledged that calmodulin binds to IQ motifs, forming a high-affinity complex even in the absence of Ca^{2+} [27]. Moreover, in the absence of Ca^{2+}, the semi-closed conformation of the C-lobe of CaM allows binding with the first part of the IQ motif (IQXXXR) [27]. Here, the hydrophobic side chain of isoleucine fits snugly into a hydrophobic pocket in calmodulin, while the glutamine establishes crucial hydrogen bonding interactions [27,28]. Consequently, it is plausible that in the absence of Ca^{2+}, CaM may bind to HRas in a non-specific manner, leading to an increase in Ras GTPase activity. This proposed mechanism provides a reasonable explanation for the observed enhancement in GTPase activity only in the presence of CaM.

Interaction between GAP/GEF with fusion Ras

To determine at which step of the Ras GTPase cycle the regulation occurred, the interactions between Ras fusion proteins and GAP or GEF individually were investigated by performing GAP and GEF dose-dependent assays (Table 1). By performing a concentration-dependent assay for GAP and GEF, the affinity between GAP and Ras or GEF and Ras was determined. This indicated which Ras-binding state, whether the GAP-binding state, GEF-binding state, or GTP-binding state, that was inhibited by binding of CaM. The GAP and GEF dose-dependent results are listed in Table 1. During the GEF dose-dependent assay, as shown in Figure 6B, the affinity of M13-HRas for GEF decreases by 4.3 fold, shifting from 7.52 µM to 31.80 µM. However, there was no significant change in the Vmax value, which remained at approximately 0.022 sec^{-1}. Conversely, the GAP affinity changed from 0.08 µM in the absence of Ca^{2+} to 0.21 µM in the presence of Ca^{2+}, an increase of approximately 2.6 fold, and the Vmax value decreased 3 fold, which was 0.006 sec^{-1} in the absence of Ca^{2+} and 0.002 sec^{-1} in the presence of Ca^{2+} (Figure 6A).

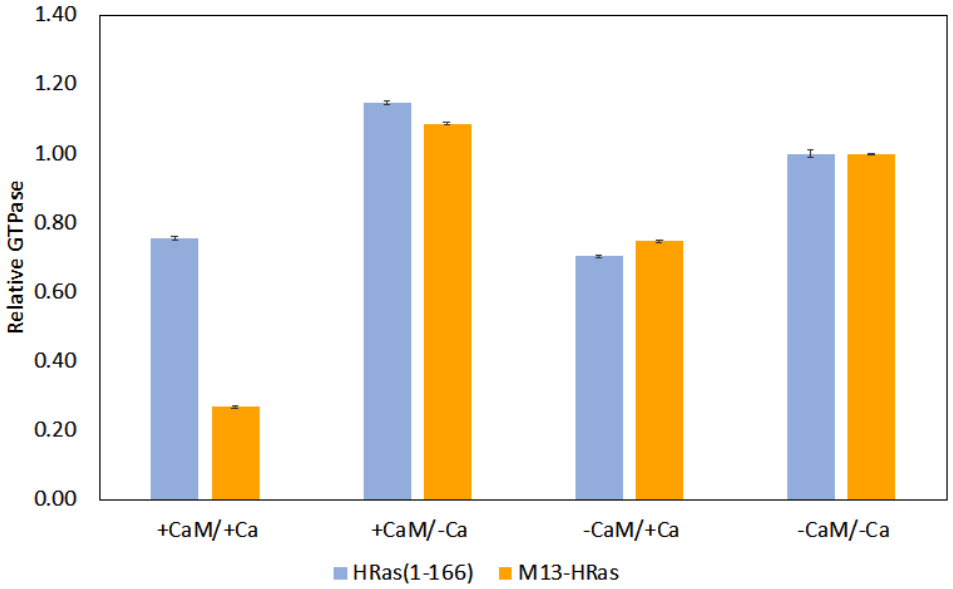

Fig. 5. Relative M13-HRas GTPase activity with ion control at 630 nm: GTPase activity of Hras (1-166), M13-HRas was measured at 25 ÚC in a reaction mixture containing 2.5µM HRas, 2.5 µM GAP, 2.5 µM GEF, 2.5 µM CaM, 0.5 mM $CaCl_2$/EDTA, 30 mM Tris-HCl (pH7.5), 120 mM NaCl, 2mM $MgCl_2$, 1 mM GTP as described previously [10]. The data and standard deviation were derived from three independent experiments

Therefore, these results suggested that the GEF and GAP affinity of M13-HRas was drastically reduced by CaM binding to M13-HRas.

To elucidate the observed decrease in GAP binding affinity to M13-HRas upon CaM binding, a plausible mechanism involves a slight yet critical displacement within the HRas GTPase catalytic site. This specific site accommodates the Arg finger of GAP, an interaction pivotal for GTPase activity [29]. The introduction of CaM is proposed to induce a subtle structural reconfiguration at the HRas Arg finger pocket. This theory is supported by research from Carsten et al., which indicates that Ras GTPase activity is highly susceptible to

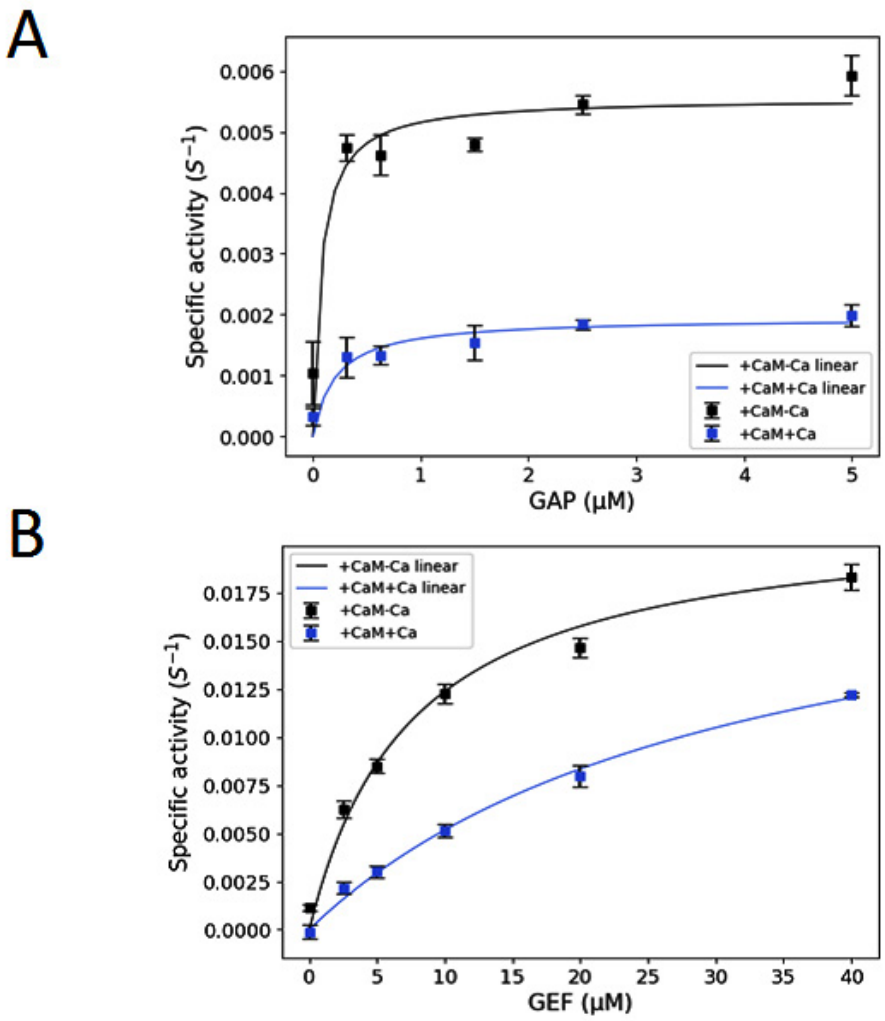

Fig. 6. Concentration dependence of the M13-HRas binding of GEF or GAP: The effect of M13-HRas ion control on GTPase activity in the presence GEF and GAP were measured in assay buffer consisting of 30 mM Tris-HCl pH7.5, 120 mM NaCl, 2 mM $MgCl_2$ and 1 mM GTP with (A) Concentration dependency of GAP was measured with 0-5 ìM GAP, 2.5 ìM GEF and 2.5 ìM M13-HRas 0.5 mM $CaCl_2$(=Øæß) or 0.5 mM EGTA(%). The solid line was the best fit for the data with a Kd of 80 nM in the absence of Ca^{2+} and a Kd of 210 nM in the presence of Ca^{2+} as described previously [10]. (B) Concentration dependency of GEF was measured with 0-40 ìM GEF, 2.5 uM GAP and 2.5 ìM M13-HRas 0.5 mM $CaCl_2$(=Øæß) or 0.5 mM EGTA(%). The solid line was the best fit for the data with a Kd of 7.52 µM in the absence of Ca^{2+} and a Kd of 31.80 µM in the presence of Ca^{2+} as described previously [10]. The data and standard deviation were derived from three independent experiments.

minimal alterations within this pocket [30]. A minor displacement, though seemingly insignificant, can disrupt the precise alignment necessary for the Arg finger of GAP to engage effectively [30]. Consequently, this misalignment significantly diminishes the catalytic efficiency of HRas by impeding the essential interaction required for GTP hydrolysis. Therefore, CaM binding to HRas not only alters the protein's conformation but also indirectly modulates its functional interaction with GAP, leading to a marked reduction in GTPase activity.

Upon meticulous examination of the three-dimensional (3D) structures of the Ras:GAP and Ras:GEF complexes, a distinctive spatial distribution of their respective binding sites within the Ras molecule was observed. The GEF binding site in Ras spanned the 23–76 amino acid (aa) region, while the GAP binding site was identified in the 11–41 aa region [31,32]. This intriguing structural insight highlighted that the GEF-binding site was situated closer to the N-terminus of Ras compared to the GAP-binding site.

Motivated by this spatial distinction, the decision was made to strategically incorporate the M13 peptide into the N-terminus of Ras as a means of fine-tuning Ras function through CaM binding. Upon a detailed comparative analysis of the 3D structures of the Ras:GAP and Ras:GEF complexes, a clear observation emerged: the Ras:GEF binding site was indeed in closer proximity to the N-terminus of HRas than the Ras:GAP binding site. This structural contrast underscored the significance of the N-terminus in mediating interactions with GEF and GAP.

Furthermore, considering that CaM, with a molecular weight of 17 kDa, is notably smaller (68%) than Ras, it was inferred that the

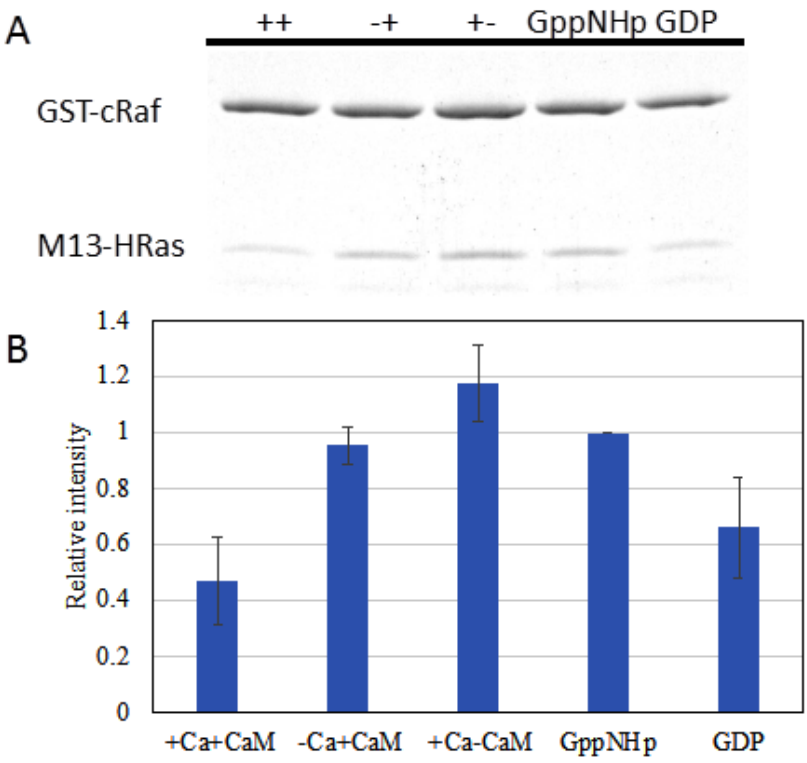

Fig. 7. Analysis of the interaction between M13-HRas and GST-cRaf : (A) Pulldown assay to show that interaction between M13-HRas and GST-Raf is inhibited by CaM binding. M13-HRas and GST-cRafwas treat with 0 or 10 μM CaM and 20 mM EGTA or 100 mM $CaCl_2$ in HEPES buffer. Then, resolved in 10% SDS-PAGE and dyed with Coomassie Brilliant Blue (CBB)-stained. (B) The intensity of each band in (A) was analyzed by ImageJ. The data and standard deviation were derived from three independent experiments

binding of CaM to the N-terminus of Ras would likely exert a more pronounced influence on the Ras:GEF binding site than on the Ras:GAP binding site [14]. This nuanced understanding of the spatial relationships within the molecular architecture provides valuable insights into the potential mechanisms underlying the regulatory effects of CaM on Ras functionality.

Interaction between Ras fusion protein and cRaf pulldown assay

This experiment was conducted to investigate whether the activity of the downstream effector Raf was affected by ion control of the fusion Ras protein. Thus, an *in vitro* binding assay was performed using GST-c-Raf (RBD) fusion protein. In the GST pull-down experiments, M13-HRas was subjected to nucleotide exchange by treating it with 5 μM EDTA and excessive GppNHp/GDP for 5 min at 30 °C and was tested using the same four steps as that of the GTPase activity assay in the presence of GppNHp. Ras-GppNHp and GDP were used as controls.

As shown in Figure 7, the presence of Ca^{2+} and CaM decreases the binding of M13-HRas to GST-Raf by approximately 62%. The region encompassing Ras amino acids 37–51 has been identified as having the maximum inhibitory effect on the association with Raf, as documented in previous studies [19]. The 3D structure analysis further reveals that this crucial region is close to the N-terminal site of Ras [33]. Consequently, when Calmodulin (CaM) binds to the M13 peptide, which has been specifically engineered at the N-terminus of Ras, there is a significant likelihood that CaM binding effectively obscures the 37–51 region. This masking action serves to inhibit the Ras/Raf association reaction, a pivotal step in the signaling pathway. The observed interaction between CaM and the modified M13-HRas suggests a consequential reduction in the activity of downstream signaling components. Such findings imply that the regulation of ion concentrations, particularly through the manipulation of CaM binding, can exert control over cellular processing

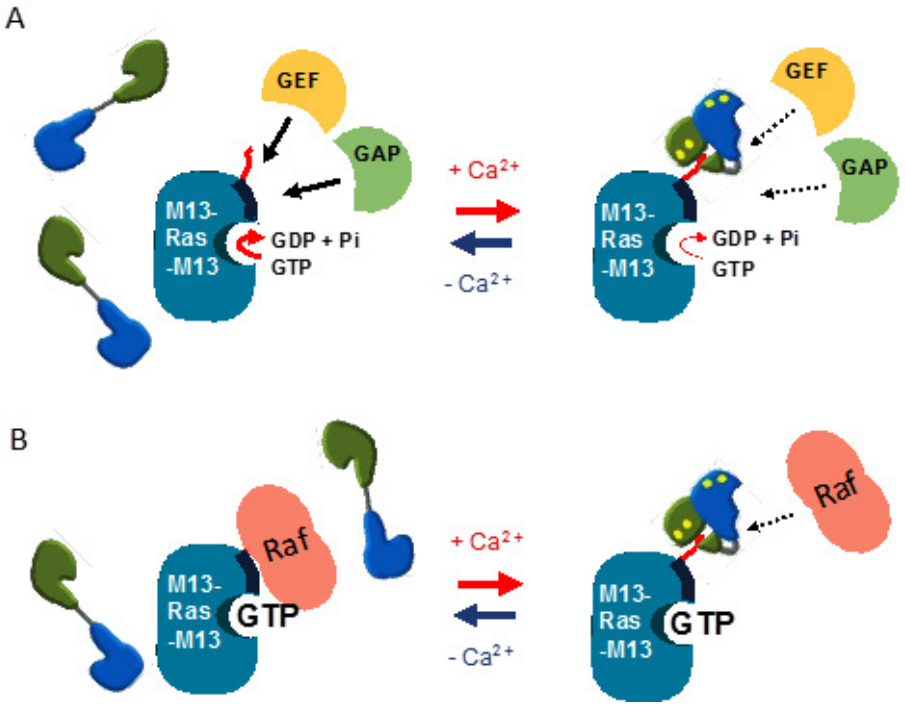

Fig. 8. Mechanism of the control of Ras using calmodulin-based iono-chromic nanodevice : (A) In the absence of Ca^{2+}, GEF and GAP could bind with Ras with no effect, however, in the presence of Ca^{2+}, CaM will bind to the incorporated M13 peptide in the N-terminus of Ras, causing a reduce in Ras:GEF and Ras:GAP binding affinity. (B) Raf can form a bond with Ras in the absence of Ca^{2+}, however, due to the binding of CaM, the amount of Ras that could bind with Raf could decrease.

mechanisms. Given Ras's pivotal role in the RAS-MAPK pathway, which is essential for cell signaling and processing, the ability to modulate its activity through ion control presents a novel approach to influencing cellular function and signaling pathways [23,34–37].

The discovery of CaM binding to modified Ras proteins has provided valuable insight into the regulatory potential of controlling Ras activity. This opens new possibilities for the development of therapeutic strategies and biotechnological applications. With this knowledge, researchers can target one of the most fundamental aspects of cell signaling, which has far-reaching implications for understanding and manipulating cellular processes.

Despite the successful in vitro regulation of Ras activity through alterations in Ca^{2+} concentration, the challenge persists in effectively controlling Ca^{2+} levels within living cells. A recent study by Chrysoula et al. (2023) has revealed a fascinating avenue for addressing this concern [38]. According to their findings, mechanostimulation in plant leaves leads to an increase in intracellular Ca^{2+} concentration, offering a potential strategy to modulate cellular conditions [38,39].

Drawing inspiration from this discovery, the prospect arises to introduce M13-HRas into plant cells, thereby leveraging the inherent mechanostimulation response to automatically regulate cell-factory processes. This innovative approach capitalizes on the natural mechanisms within plant cells, providing a promising solution to the intricate task of dynamically controlling Ca^{2+} concentrations in a living cellular environment.

This intriguing intersection of mechanostimulation, Ras regulation, and plant cell physiology holds potential implications for advancing the field of automatic cell-factory processing. By tapping into the cellular responses triggered by mechanostimulation, this approach may pave the way for enhanced precision and efficiency in biotechnological applications within plant cells.

CONCLUSIONS

This study presents a successful methodology for modulating the activity of the small GTPase protein Ras by introducing an M13 peptide into its functional site. The GTPase activity of Ras exhibited a substantial reduction of 73% in the presence of Ca^{2+} compared to its activity in the absence of Ca^{2+}. Dose-dependent assays involving GTPase-activating proteins (GAP) and guanine nucleotide exchange factors (GEF) revealed a significant decrease in Ras:GEF binding affinity and a slight reduction in Ras:GAP binding affinity upon CaM binding, as illustrated in Figure 8A. These findings were further validated through comprehensive 3D structural analyses.

Moreover, the inhibition of Ras:Raf binding by GTPase activity was demonstrated, emphasizing the impact of CaM binding on downstream protein interactions (Figure 8B). While acknowledging the in vitro nature of this study, its outcomes propose a potential avenue for manipulating G protein functionality through variations in Ca^{2+} concentration. This discovery holds promising implications for future applications in automated cell-factory processes and cancer therapy.

ACKNOWLEDGMENTS

We would like to thank Dr. Alrazi and Dr. Kondo for helpful discussion and comments on this study.

Conflict of Interest

The authors declare no conflict of interest.

Funding Sources

Scientific Research Grant from Soka University. inactive. GEFs expedite the conversion of the inactive GDP to its active GTP counterpart, while GAPs hasten the hydrolysis of GTP, causing it to revert to its inactive state.

REFERENCES

1. Sadakane, K., Takaichi, M. & Maruta, S. Photocontrol of the mitotic kinesin Eg5 using a novel photochromic inhibitor composed of a spiropyran derivative. *J. Biochem. (Tokyo)* 164, 239–246 (2018).
2. Alrazi, I. M., Sadakane, K. & Maruta, S. Novel photochromic inhibitor for mitotic kinesin Eg5 which forms multiple isomerization states. *J. Biochem. (Tokyo)* 170, 229–237 (2021).
3. Gasper, R. & Wittinghofer, F. The Ras switch in structural and historical perspective. *Biol. Chem.* 401, 143–163 (2019).
4. Tchernitsa, O. I. *et al.* Transcriptional basis of KRAS oncogene-mediated cellular

transformation in ovarian epithelial cells. *Oncogene* 23, 4536–4555 (2004).
5. Wittinghofer, A., Scheffzek, K. & Ahmadian, M. R. The interaction of Ras with GTPase-activating proteins. *FEBS Lett.* 410, 63–67 (1997).
6. New, D. C. & Wong, Y. H. Molecular mechanisms mediating the G protein-coupled receptor regulation of cell cycle progression. *J. Mol. Signal.* 2, 2 (2007).
7. Tamada, M., Hu, C.-D., Kariya, K., Okada, T. & Kataoka, T. Membrane recruitment of Raf-1 is not the only function of Ras in Raf-1 activation. *Oncogene* 15, 2959–2964 (1997).
8. Marshall, C. J. Ras effectors. *Curr. Opin. Cell Biol.* 8, 197–204 (1996).
9. Nahar, R. *et al.* Multimerization of small G-protein H-Ras induced by chemical modification at hyper variable region with caged compound. *J. Biochem. (Tokyo)* 171, 215–225 (2022).
10. Feringa, B.L. (ed): Molecular Switches. Weinheim; Chichester: Wiley-VCH (2001).
11. Liu, Y., Duan, Z.-Y., Zhang, H.-Y., Jiang, X.-L. & Han, J.-R. Selective Binding and Inverse Fluorescent Behavior of Magnesium Ion by Podand Possessing Plural Imidazo[4,5-f]-1,10-phenanthroline Groups and Its Ru(II) Complex. *J. Org. Chem.* 70, 1450–1455 (2005).
12. Chin, D. & Means, A. R. Calmodulin: a prototypical calcium sensor. *Trends Cell Biol.* 10, 322–328 (2000).
13. Tidow, H. & Nissen, P. Structural diversity of calmodulin binding to its target sites. *FEBS J.* 280, 5551–5565 (2013).
14. Kim, J. *et al*. Calmodulin mediates Ca2+ sensitivity of sodium channels. *J. Biol. Chem.* 279, 45004–45012 (2004).
15. Andrews, C., Xu, Y., Kirberger, M. & Yang, J. J. Structural Aspects and Prediction of Calmodulin-Binding Proteins. *Int. J. Mol. Sci.* 22, 308 (2020).
16. Meador, W. E., Means, A. R. & Quiocho, F. A. Target Enzyme Recognition by Calmodulin: 2.4 Å Structure of a Calmodulin-Peptide Complex. *Science* 257, 1251–1255 (1992).
17. Blumenthal, D. K. *et al.* Identification of the calmodulin-binding domain of skeletal muscle myosin light chain kinase. *Proc. Natl. Acad. Sci. U. S. A.* 82, 3187–3191 (1985).
18. Bayley, P. m., Findlay, W. a. & Martin, S. r. Target recognition by calmodulin: Dissecting the kinetics and affinity of interaction using short peptide sequences. *Protein Sci.* 5, 1215–1228 (1996).
19. Barnard, D. *et al*. Identification of the sites of interaction between c-Raf-1 and Ras-GTP. *Oncogene* 10, 1283–1290 (1995).
20. Shishido, H., Nakazato, K., Katayama, E., Chaen, S. & Maruta, S. Kinesin-Calmodulin fusion protein as a molecular shuttle. *J. Biochem. (Tokyo)* 147, 213–223 (2010).
21. Nahar, R., A, A. M. N., Alrazi, I. M. & Maruta, S. Photocontrol of GTPase Cycle and Multimerization of the Small G-Protein H-Ras using Photochromic Azobenzene Derivatives. *Biosci. Biotechnol. Res. Asia* 18, 661–672 (2021).
22. Nishibe, N. & Maruta, S. Photocontrol of small GTPase Ras fused with a photoresponsive protein. *J. Biochem. (Tokyo)* mvae017 (2024) doi:10.1093/jb/mvae017.
23. Bourne, H. R., Sanders, D. A. & McCormick, F. The GTPase superfamily: conserved structure and molecular mechanism. *Nature* 349, 117–127 (1991).
24. Green, D. F., Dennis, A. T., Fam, P. S., Tidor, B. & Jasanoff, A. Rational design of new binding specificity by simultaneous mutagenesis of calmodulin and a target peptide. *Biochemistry* 45, 12547–12559 (2006).
25. Buhrman, G., Holzapfel, G., Fetics, S. & Mattos, C. Allosteric modulation of Ras positions Q61 for a direct role in catalysis. *Proc. Natl. Acad. Sci. U. S. A.* 107, 4931–4936 (2010).
26. O'Connor, C. & Kovrigin, E. L. Characterization of the second ion-binding site in the G domain of H-Ras. *Biochemistry* 51, 9638–9646 (2012).
27. Trybus, K. M. *et al*. Effect of Calcium on Calmodulin Bound to the IQ Motifs of Myosin V*. *J. Biol. Chem.* 282, 23316–23325 (2007).
28. Fallon, J. L., Halling, D. B., Hamilton, S. L. & Quiocho, F. A. Structure of Calmodulin Bound to the Hydrophobic IQ Domain of the Cardiac Cav1.2 Calcium Channel. *Structure* 13, 1881–1886 (2005).
29. Gerwert, K., Mann, D. & Kötting, C. Common mechanisms of catalysis in small and heterotrimeric GTPases and their respective GAPs. *Biol. Chem.* 398, 523–533 (2017).
30. Kötting, C., Kallenbach, A., Suveyzdis, Y., Wittinghofer, A. & Gerwert, K. The GAP arginine finger movement into the catalytic site of Ras increases the activation entropy. *Proc. Natl. Acad. Sci.* 105, 6260–6265 (2008).
31. Hodges, T. R. *et al.* Discovery and Structure-Based Optimization of Benzimidazole-Derived Activators of SOS1-Mediated Nucleotide Exchange on RAS. *J. Med. Chem.* 61, 8875–8894 (2018).
32. Scheffzek, K. *et al.* The Ras-RasGAP complex: structural basis for GTPase activation and its loss in oncogenic Ras mutants. *Science* 277, 333–338 (1997).
33. Park, E. *et al.* Cryo-EM structure of a RAS/RAF recruitment complex. *Nat. Commun.* 14, 4580

(2023).
34. Aoki, Y. & Matsubara, Y. Human development and the RAS/MAPK pathway. *Seikagaku* 79, 34–38 (2007).
35. Joneson, T. & Bar-Sagi, D. Ras effectors and their role in mitogenesis and oncogenesis. *J. Mol. Med.* 75, 587–593 (1997).
36. Han, C. W., Jeong, M. S. & Jang, S. B. Structure, signaling and the drug discovery of the Ras oncogene protein. *BMB Rep.* 50, 355–360 (2017).
37. Molina, J. R. & Adjei, A. A. The Ras/Raf/MAPK Pathway. *J. Thorac. Oncol.* 1, 7–9 (2006).
38. Pantazopoulou, C. K. *et al.* Mechanodetection of neighbor plants elicits adaptive leaf movements through calcium dynamics. *Nat. Commun.* 14, 5827 (2023).
39. Palzkill, D. & Tibbitts, T. Evidence That Root Pressure Flow Is Required for Calcium Transport to Head Leaves of Cabbage. *Plant Physiol.* 60, 854–6 (1978).